A camera-based system for highly accurate 3D displacement field measurement and contactless force sensing

[1]Debbie Zhao, [1]Amir HajiRassouliha, [1]Emily J. Lam Po Tang, [1,2]Martyn P. Nash, [1,2]Poul M. F. Nielsen, and [1,2]Andrew J. Taberner

[1]Auckland Bioengineering Institute, [2]Department of Engineering Science,
The University of Auckland, Auckland, New Zealand
amir.hajirassouliha@auckland.ac.nz

Abstract—Recent advances in digital image correlation (DIC) techniques now enable full-field measurements of surface shape and deformation using relatively inexpensive camera systems. Yet, established methods are not without limitations, exhibiting only modest accuracy and considerable sensitivity to noise effects. In order to address this, we have developed an advanced computer vision toolbox with which it is possible to accurately detect three-dimensional (3D) surface displacements to a practical resolution of 10 µm over a field of view of approximately 150 mm × 150 mm. By taking advantage of a high-resolution subpixel image registration algorithm and a stereoscopic imaging system, a methodological basis for a highly accurate and comprehensive deformation analysis is presented. This was demonstrated by the application of known forces to a simple cantilever structure while measuring resultant surface deformations. Measurements were then compared with expected displacement values predicted by analytical calculations as well as a finite element model. Comparisons showed our measurements were within 120 µm of model predictions. Subsequently, we propose a method of non-contact force-sensing by exploiting the relationship between known applied forces and acquired displacement data. For our dataset, the system was able to predict force to within 0.38 %.

Keywords—*digital image correlation (DIC), experimental mechanics, stereoscopy, displacement measurement, force measurement*

I. Introduction

To date, digital image correlation (DIC) techniques have been widely applied in experimental characterisation of the shape and deformation of materials and structures. This class of techniques involves the use of an optical measurement system in which images of a target undergoing structural change are computationally processed to determine the corresponding surface deformation. These techniques provide the advantage of being non-specific in terms of the expected material and deformation characteristics (i.e. including, but not limited to compression, torsion, or bending), and thus have a wide variety of engineering and non-engineering applications. Accordingly, DIC techniques have since been described as fomenting a 'revolution in experimental mechanics' (Reu [1]). Where once single point displacement and strain measurements were the standard, DIC can instead provide full-field information. By comparing sequential digital images of an object surface in the reference and deformed states, it is possible to not only observe structural contour and object deformation, but from such data derive further components such as modes of vibration [2], strain fields [3], and measure how these may vary across geometry and time. The capability of DIC techniques in accurately characterising material behaviour and the response of structures to external loads has, in many cases, provided a more complete understanding of the underlying mechanics.

While two-dimensional (2D) DIC measurement systems may be appropriate for many applications from tensile testing [4], [5] and studies of crack propagation [6]–[8], to deformation mapping for biomedical images [9]–[11], they might be insufficient in circumstances where the object undergoes complex and/or out of plane deformations. By simultaneously recording images of an overlapping field of view using two or more cameras from different viewpoints, it is possible to analyse the surface of an object in 3D space. Thus, the use of DIC in a stereoscopic imaging system extends measurements into the 3D domain to permit more complex analyses.

The measurement of force and strain is an area that can benefit from full-field information. The measurement of force preludes many applications in bioengineering, including biomechanics [12] and monitoring of human activities [13]. Some of the modern conventional sensors include fibre optic sensors [12], wearable and smart fabric sensors [13], [14], a piezomagnetic film sensor [15], and a flexible three-axial sensor [16]. Image-based sensors are a type of modern sensors that have the advantage of being non-contact, but have only been used in a few applications, such as cardiac catheterization [17]. Among image-based techniques, 3D DIC is the most suitable technique able to provide an image-based sensor with comprehensive data from the surface deformation of the object.

However, the accuracy and robustness of DIC measurements have limited their use in many applications. Any practical application of DIC is inherently susceptible to inaccuracies due to illumination fluctuations, poorly textured surfaces, and image noise [18]. In view of these limitations, we have developed a subpixel image registration algorithm (HajiRassouliha et al. [19]) with high accuracy and robustness to noise suitable for use in DIC applications. The algorithm of HajiRassouliha et al. [19] is a two-step method that finds integer shifts using Savitzky-Golay differentiators in gradient correlation and finds subpixel shifts using a phase-based method. The resolutions of this algorithm was on the order of millipixels for actual camera measurements (i.e. non-synthetic shifts) [20]. The subpixel image registration method of HajiRassouliha et al. [19] has been validated for estimating rigid body translations, and

subsequently applied to 2D measurement of soft material deformation [20].

In this paper, we take advantage of the capabilities of the image registration method of HajiRassouliha et al. [19] to develop an accurate and robust DIC technique. The multi-camera calibration method of HajiRassouliha et al. [21] was used to extend 2D measurements to 3D DIC measurements. The 3D deformation measurements were the basis of a novel image-based force sensor. It is important to note that the aim of this paper is not to provide yet another extensive review on the capabilities of DIC, nor to comprehensively cover the implementation of the algorithm (for which the reader is referred to [19]), but rather to present an interesting feasibility study for a new application of DIC. We here propose an intuitive, yet novel, force prediction system using full-field DIC displacement data. We demonstrate firstly, the use of a simple stereoscopic imaging system, coupled with a powerful subpixel image registration algorithm, to measure the 3D deformation of the surface of a cantilever under increasing loads. Consequently, the force which gave rise to a particular deformation could then be estimated from the measured displacement field.

II. METHOD

A. Experimental Setup

To test this proposed method, we constructed a cantilever from black acrylic, as shown in Fig. 1. A load (F) was applied vertically to the free end of the cantilever by hanging standard weights on Kevlar thread secured via a bead through a 0.2 mm radius hole. The opposing (fixed) end of the cantilever was securely clamped between clear acrylic plates to a flat horizontal surface, as shown in Fig. 1. The use of a simple structure with well-characterized deformation characteristics provided a predictable displacement field with well-understood behavior.

To increase image texture for enhanced detection and processing, white ink speckle patterning was manually applied to the beam surface using an airbrush.
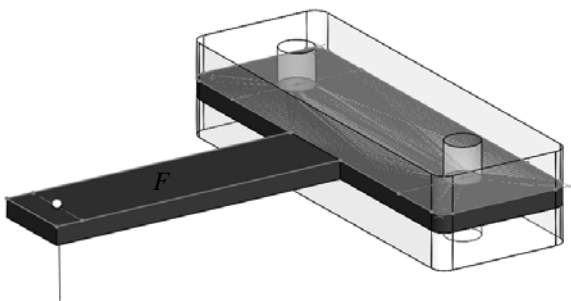

Fig. 1. Experimental setup of cantilever test structure showing clamped end (and pinholes for alignment) and beaded Kevlar thread for force application.

The experimental cantilever was constructed with the following dimensions, given in Tab. 1:

TABLE I. ACRYLIC CANTILEVER PARAMETERS

	Unit	Value
Beam Length (L)	m	0.040
Beam Width (b)	m	0.012
Beam Thickness (h)	m	0.003
Elastic Modulus (E)	N/m^2	3.0×10^9
2nd Moment of Inertia (I)	m^4	2.7×10^{-11}

As derived from the classical problem of the small displacement elastic cantilever, the maximum deflection δ_{max} (occurring at the free end) for a given load F (N) is given by:

$$\delta_{max} = \frac{FL^3}{3EI} \text{ (where } I = \frac{bh^3}{12}\text{)} \tag{1}$$

Loading steps were selected based upon prior knowledge of the practical resolution of the algorithm in detecting displacements (~1 µm over an approximate field of view of 150 mm × 150 mm, under ideal lighting conditions [20]), and the maximum load was restricted by the material yield stress (4.5×10^7 N/m^2 for Acrylic). Accordingly, force was applied by hanging masses in ten 0.100 kg increments up to 1.000 kg (i.e. between 0.981 N and 9.81 N) to satisfy these conditions.

B. Measurement Environment

A stereoscopic imaging system was assembled using two USB3 cameras (GS3-U3-32S4M-C, Point Grey) with 3.45 µm pixel size and 2048 pixel × 1536 pixel resolution, paired with 16 mm f/1.4 lenses (M118FM16, Tamron). The cameras were mounted to adjustable tripods placed approximately 80 mm from the cantilever surface, ensuring that the target was visible in both cameras under ambient lighting (see Fig. 2).

In order to perform stereoscopic measurements, a multi-camera calibration protocol [21] was conducted to identify the intrinsic parameters (which relate an object to its image) and extrinsic parameters (which define the 3D positions of each camera in a global coordinate system). This process required approximately 70 image sets to be taken of a classical checkerboard calibration template.

After successful calibration, static images from both cameras were taken simultaneously, firstly of the unloaded cantilever, and subsequently at each of the ten loading steps (producing a total of eleven image sets) for processing.
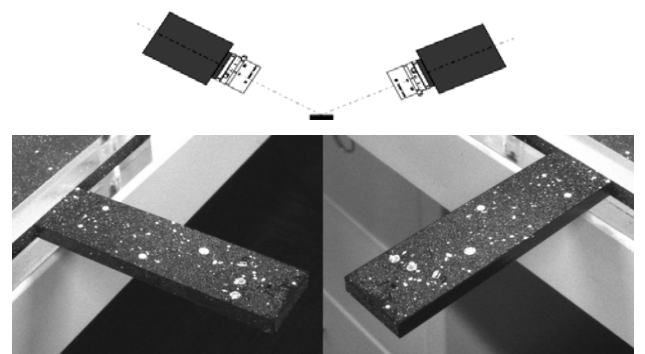

Fig. 2. Diagram showing arbitrary camera angles (approximately 120 °) and positioning from unloaded cantilever surface (top) and resultant camera views (bottom). The overlapping field of view is approximately 40 mm × 60 mm.

C. Image Processing

Material points of the cantilever surface were automatically matched between images (on subimages of size 64 pixel × 64 pixel) using the subpixel registration algorithm detailed in [19]. Corresponding 3D point locations were found by triangulation of matched points using previously found camera parameters from the multi-camera calibration process [21]. Lastly, displacements were calculated by tracking material points in 3D space across image sets.

All computations were implemented in Matlab (v16, Mathworks, Natick MA, USA), and were performed using a single thread of an Intel® 4th generation Core™ i7 CPU on a PC running Windows7 (Dell Optiplex 9020).

D. Force Calibration and Estimation

To use the system for force measurement, a second calibration process was carried out, this time to determine the relationship between the applied force and the measured displacement field. In order to use the measured full-field data, the following steps were taken:

1. The 3D displacement field was measured for approximately 105,000 points distributed over the cantilever surface at loads of 0.200 kg, 0.400 kg, 0.600 kg, 0.800 kg and 1.000 kg. The measurements were used in form of a function of applied force versus 3D displacements.

2. A second order polynomial function was fit to each of the ~105,000 displacement estimates in Step 1 (i.e. each tracked material point) as a function of the calibration loads.

3. The material points undergo different deformations depending on where they are located on the cantilever surface. To relate the deformation field to the applied force, the fits obtained in Step 2 were combined using a linear weighted averaging scheme. The weight for each material point fit was proportional to its sensitivity to the displacement measurements (i.e. slope of the displacement versus load relationship). This weighting scheme results in more significant effect from the points at the free end of the cantilever with larger displacements as they are less sensitive to image noise.

4. After finding the calibration parameters, the deformation fields measured at applied loads of 0.100 kg, 0.300 kg, 0.500 kg, 0.700 kg and 0.900 kg were used to test the accuracy of the estimated force.

5. The error of measurements was observed as a percentage of full loading range (i.e. of 1.000 kg, for which the system was calibrated).

E. Comparison of the measurements with analytical measurements

The 3D measurements obtained from the stereoscopic system were compared with both analytical predictions (i.e. calculated using (1)) and a computational finite element (FE)

model generated using SolidWorks Simulation ®. The purpose of using the analytical and FE models was to provide data on the expected deformation values as they are well-known methods of measuring deformations. The accuracy of the subpixel deformation measurement algorithm as the core part of the method of this paper has been validated in previous studies [20], [22].

Please note that the measurements from the stereoscope shall not exactly match the expected measurements due to the unideal nature of the cantilever beam and practical limitations of the experiment.

III. RESULTS

A. Surface Reconstruction

The cantilever surface was successfully reconstructed for all eleven image sets as exemplified in Fig. 3, with approximately 105,000 points on the object surface in 3D coordinates. Each 3D reconstruction took approximately 15 minutes to compute.

Fig. 3. 3D reconstructions of the speckled cantilever surface showing undeformed (0 N, top) and deformed state (9.81 N, bottom).

B. Displacement Measurements

A FE model of the cantilever beam (Fig. 4) was created, complete with material settings and appropriate fixtures and loads. The geometry under analysis was then discretised using tetrahedral, triangular, and beam elements, and solved using the displacement formulation to calculate the resultant deformation. This permitted qualitative observations of the surface deformation pattern of the model upon loading, as well as quantitative analyses of displacement magnitudes across both model geometry and loading steps. This can be visually compared with Fig. 5, which demonstrates the ability of the system to resolve the displacement field of the cantilever to ~1 µm resolution, where a gradient of displacements is also apparent across the length of the beam.
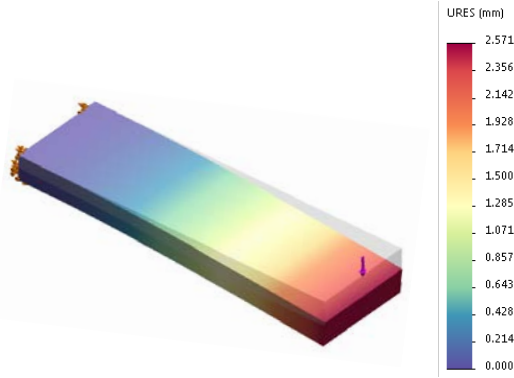
Fig. 4. Finite element simulation of cantilever beam showing displacements at maximum loading (P = 9.81 N).

Table 2 shows the comparison between the measured displacements with both analytical predictions and a computational FE model. To simplify the process, the comparisons were performed only at the free end of the cantilever (δ_{max}). This eliminated the need to generate an error metric for appropriate quantification over the entire cantilever surface (where, perhaps, points closer to the free end may incur more heavily weighted error). In regards to surface deformation, extracted data points from the free end alone are sufficient in demonstrating the ability to produce accurate displacement measurements. However, in estimating the force applied, it is important to note again that full-field data (i.e. every data point) was utilised in the calculation described in the methods section.
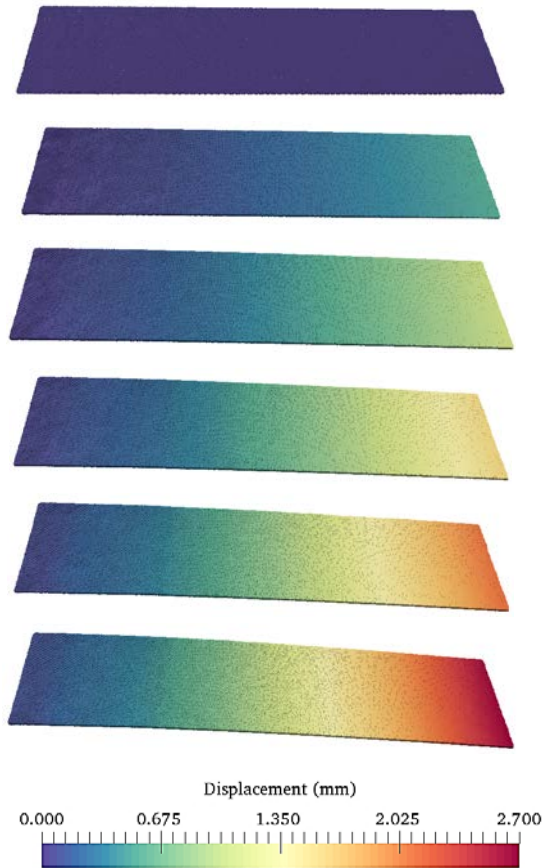

Fig. 5. Measured displacement field across cantilever surface with increased loading (P = 0 N, 1.96 N, 3.92 N, 5.89 N, 7.85 N and 9.81 N are shown in ascending order).

The errors in Tab. 2 represent the difference in displacement magnitude between the stereoscopic DIC measurements and the analytical and FE models.

TABLE II.   COMPARISON OF DISPLACEMENTS

Load (kg)	Displacements (mm)				
	Stereoscopic DIC	Analytical		FE Model	
		Value	Error	Value	Error
0.100	0.242	0.258	**-0.016**	0.253	**-0.011**
0.200	0.495	0.517	**-0.022**	0.505	**-0.010**
0.300	0.754	0.775	**-0.021**	0.758	**-0.004**
0.400	1.015	1.033	**-0.018**	1.011	**0.004**
0.500	1.275	1.292	**-0.017**	1.265	**0.010**
0.600	1.547	1.550	**-0.003**	1.518	**0.029**
0.700	1.825	1.809	**0.016**	1.771	**0.054**
0.800	2.085	2.067	**0.018**	2.024	**0.061**
0.900	2.369	2.325	**0.044**	2.277	**0.092**
1.000	2.644	2.584	**0.060**	2.530	**0.114**

C. Force Prediction

Tab. 3 shows predictions of force using the proposed method and the associated errors in comparison to the true applied load.

TABLE III.   STEREOSCOPIC DIC FORCE PREDICTIONS AND ESTIMATION ERRORS

Load (kg)		Error	
Applied	Predicted	kg	% [a]
0.100	0.0968	-0.0032	0.32
0.300	0.3008	0.0008	0.08
0.500	0.4996	-0.0004	0.04
0.700	0.7038	0.0038	0.38
0.900	0.9018	0.0018	0.18

[a.] Percentage of full loading range (i.e. of 1.000 kg)

IV. DISCUSSION

Using a simple cantilever structure we were able to demonstrate the use of a stereoscopic DIC system in measuring full-field 3D surface deformations of a cantilever with a resolution of the order of ~1 µm. Upon comparison of measured data to analytic and FE model solutions, displacements were consistently within 0.114 mm across all loading steps, suggesting valid measurements. The largest discrepancy of 0.114 mm (refer to Tab. 2, last row and column) was found between the FE model and stereoscopic DIC at maximum loading over a displacement range of 2.6 mm. It is not easily feasible to find what portion of this error is caused by our method since the model predictions assume ideal and well-known material behavior and linearity, which is often not the case in practical measurement applications.

From (1), it is apparent that the confidence in beam dimensions is critical to the analytical result—as both L and h are cubed, any discrepancies in these measurements would result in reasonably significant error. For instance, nominally 3 mm acrylic can in practice be between 2.9 mm and 3.1 mm due to manufacturing processes.

While the process demonstrated in this report fulfils that of a simple structure under controlled conditions, the procedure may be easily extended to more complex structures and loading conditions. A more powerful result could also be obtained by comparing point displacements over the entire cantilever with respect to its geometry (as full-field information is available for both DIC measurements and the FE model). Additionally, our system is able to respond to practical sources of error (inclusive of imperfect fixtures or load distribution potentially altering resultant object deformations) in the experimental method which are difficult to predict with a FE model. Where FE approaches offer static solutions specific to predefined conditions, DIC in turn presents a dynamic alternative; one that is reflective of the structural deformation problem which is fundamentally non-static.

By utilizing the high quality of our full-field data, we have subsequently demonstrated the feasibility of using our stereoscopic DIC system as a means of a robust, non-contact, optical force-sensing. The advantage of such an approach is that it is independent of material geometry and material law constitutive parameters, provided that an appropriate calibration has been performed. This in turn eliminates the need for certain model assumptions, which may lead to incorrect calculations or bias in results. We have thus far tested a very simple implementation based on only five calibration points, which returned a prediction to within 0.38 % of the measurement range (refer to Tab. 3). The precision of this procedure could be further improved through methodological design, such as increasing the number of calibration steps or pre-processing (e.g. smoothing) of displacement data. Further investigations are also needed to determine the effects of factors such as goodness of fit (between displacement data and applied forces) during calibration and the method of assigning weights to produce an optimal force prediction.

Given the high resolution provided by the algorithm, it is apparent that information may become redundant across the full-field data. Thus, it may be sensible to down-sample material points (depending on the deformation characteristics) to decrease the required processing time (current measurements are based on approximately 105,000 points). Similarly, it would be interesting to investigate the effectiveness of using a single camera in complement with a classical 2D implementation of DIC which would again, significantly reduce computational expenditure. To enable real-time implementations of this method, we are also presently developing a hardware accelerated version and parallel implementation of our algorithm, using field programmable gate arrays and graphical processing units.

Finally, although it has been demonstrated here that force may be back-calculated from displacement data, this methodology is by no means restricted to this variable. In principle, the same measurement system could be applied to any sensor that converts a measurement quantity in to a displacement field (e.g. pressure, velocity, and temperature change), provided that an appropriate calibration has been carried out. The availability of such a framework consequently presents a new opportunity, for which conventional sensing methods may prove to be a challenge in terms of experimental implementations.

V. Conclusions

In this paper, we successfully demonstrated the feasibility of using a stereoscopic DIC system as a means of force prediction, providing an innovative metrological framework for contactless sensing. The 3D surface geometries and deformation were precisely resolved on the order of approximately 1 μm over an approximate field of view of 40 mm × 60 mm using our 3D DIC technique (4×10^{-5} % of the area). The 3D measurements by our stereoscopic DIC system closely resembled FE model predictions, with a maximum discrepancy of 0.114 mm over a 2.6 mm range for the cantilever beam used in this experiment. The 3D measurements then were used to predict the force applied to the cantilever beam where force predictions were accurate to within 0.38 % of the full calibrated range (9.81 N).

As an adjunct to the continuous development and growing interest in DIC technology, our solution presents an adaptable tool for deformation analysis and for the first time—a means of contactless force prediction through advanced image analysis.

References

[1]   P. Reu, "DIC: A Revolution in Experimental Mechanics," *Experimental Techniques*, vol. 39, no. 6, pp. 1–2, 2015.

[2]   A. Yashar, N. Ferguson, and M. G. Tehrani, "Measurement of rotating beam vibration using optical (DIC) techniques," in *Procedia Engineering*, 2017, vol. 199, pp. 477–482.

[3]   B. Pan, "Full-field strain measurement using a two-dimensional Savitzky-Golay digital differentiator in digital image correlation," *Opt. Eng.*, vol. 46, no. 3, p. 033601, 2007.

[4]   S. Hartmann, R. R. Gilbert, and C. Sguazzo, "Basic studies in biaxial tensile tests," *GAMM Mitteilungen*, 2018.

[5]   X. Li, W. Xu, M. A. Sutton, and M. Mello, "In Situ nanoscale In-plane deformation studies of ultrathin polymeric films during tensile deformation using atomic force microscopy and digital image correlation techniques," *IEEE Trans. Nanotechnol.*, 2007.

[6]   G. Gonzales, J. A. González, V. Paiva, and J. Freire, *Crack-Tip Plastic Zone Size and Shape via DIC: Proceedings of the 2018 Annual Conference on Experimental and Applied Mechanics*. 2019.

[7]   S. H. Tung and C. H. Sui, "Application of digital-image-correlation techniques in analysing cracked cylindrical pipes," *Sadhana - Acad. Proc. Eng. Sci.*, 2010.

[8]   M. Ghahremannejad, M. Mahdavi, A. E. Saleh, S. Abhaee, and A. Abolmaali, "Experimental investigation and identification of single and multiple cracks in synthetic fiber concrete beams," *Case Stud. Constr. Mater.*, 2018.

[9]   J. S. Affagard, P. Feissel, and S. F. Bensamoun, "Measurement of the quadriceps muscle displacement and strain fields with ultrasound and Digital Image Correlation (DIC) techniques," *IRBM*, 2015.

[10]   Z. Chen, W. Lenthe, J. C. Stinville, M. Echlin, T. M. Pollock, and S. Daly, "High-Resolution Deformation Mapping Across Large Fields

of View Using Scanning Electron Microscopy and Digital Image Correlation," *Exp. Mech.*, vol. 58, no. 9, pp. 1407–1421, 2018.

[11] K. Kamiyama, M. Mikuni, and T. Matsumoto, "Fracture propagation analysis on two component type acrylic adhesive joints," *Int. J. Adhes. Adhes.*, vol. 83, pp. 76–86, 2018.

[12] P. Roriz, L. Carvalho, O. Frazão, J. L. Santos, and J. A. Simões, "From conventional sensors to fibre optic sensors for strain and force measurements in biomechanics applications: A review," *J. Biomech.*, vol. 47, no. 6, pp. 1251–1261, 2014.

[13] S. C. Mukhopadhyay, "Wearable Sensors for Human Activity Monitoring: A Review," *IEEE Sens. J.*, vol. 15, no. 3, pp. 1321–1330, Mar. 2015.

[14] L. M. Castano and A. B. Flatau, "Smart fabric sensors and e-textile technologies: A review," *Smart Mater. Struct.*, vol. 23, no. 5, 2014.

[15] Q. Lin, Z. Zhu, J. Chen, D. Liu, and H. Zhao, "A new piezomagnetic film force sensor model for static and dynamic stress measurements," *J. Magn. Magn. Mater.*, vol. 466, no. June, pp. 106–111, 2018.

[16] L. Viry *et al.*, "Flexible three-axial force sensor for soft and highly sensitive artificial touch," *Adv. Mater.*, vol. 26, no. 17, pp. 2659–2664, 2014.

[17] Y. Noh *et al.*, "Image-based optical miniaturized three-axis force sensor for cardiac catheterization," *IEEE Sens. J.*, vol. 16, no. 22, pp. 7924–7932, 2016.

[18] D. Medvedofsky *et al.*, "Three-Dimensional Echocardiographic Automated Quantification of Left Heart Chamber Volumes Using an Adaptive Analytics Algorithm: Feasibility and Impact of Image Quality in Nonselected Patients," *J. Am. Soc. Echocardiogr.*, vol. 30, no. 9, 2017.

[19] A. HajiRassouliha, A. J. Taberner, M. P. Nash, and P. M. F. Nielsen, "Subpixel phase-based image registration using Savitzky-Golay differentiators in gradient-correlation," *Computer Vision and Image Understanding*, 2017.

[20] A. HajiRassouliha, A. J. Taberner, M. P. Nash, and P. M. F. Nielsen, "Subpixel measurement of living skin deformation using intrinsic features," in *Proceedings of Computational Biomechanics for Medicine XI Workshop, MICCAI*, 2016.

[21] A. HajiRassouliha, A. J. Taberner, M. P. Nash, and P. M. F. Nielsen, "Robust and accurate multiple camera stereographic calibration."

[22] A. HajiRassouliha, A. J. Taberner, M. P. Nash, and P. M. F. Nielsen, "Motion correction using subpixel image registration," in *Proceedings of International Workshop on Reconstruction and Analysis of Moving Body Organs, MICCAI*, 2017, pp. 14–23.